Brain, Behavior, & Immunity - Health 7 (2020) 100110

Contents lists available at ScienceDirect

Brain, Behavior, & Immunity - Health

journal homepage: www.editorialmanager.com/bbih/default.aspx

Full Length Article

Developmental ablation of mature oligodendrocytes exacerbates adult CNS demyelination

Ahdeah Pajoohesh-Ganji *, Molly Karl, Eric Garrison, Nana Adwoa Osei-Bonsu, Cheryl Clarkson-Paredes, Julie Ahn, Robert H. Miller

Department of Anatomy and Cell Biology, The George Washington University, School of Medicine and Health Sciences, Washington, DC, United States

ARTICLE INFO

Keywords:
Multiple sclerosis
LPC
EAE
Priming
Inflammation

ABSTRACT

Multiple sclerosis (MS) is a CNS neurodegenerative autoimmune disease characterized by loss of oligodendrocytes and myelin in the brain and the spinal cord that results in localized functional deficits. Several risk factors have been associated with MS, however none fully explain the enhanced susceptibility seen in older individuals. Epidemiological data, based on geographical prevalence studies suggest that susceptibility is established early in life and frequently long before the diagnosis of disease raising the possibility that developmental events influence adult disease onset and progression. Here we test the hypothesis that selective loss of mature oligodendrocytes during postnatal development results in enhanced susceptibility to a demyelinating insult to the mature CNS. A transgenic mouse model was utilized to specifically induce apoptotic cell death in a subset of mature oligodendrocytes (MBP-iCP9) during the first 2 postnatal weeks followed by either a local LPC spinal cord injection or the induction of EAE in the adult animal. Immunostaining, immunoblotting, behavioral testing, and electron microscopy were utilized to examine the differences in the response between animals with developmental loss of oligodendrocytes and controls. We show that during development, oligodendrocyte apoptosis results in transient reductions in myelination and functional deficits that recover after 10–14 days. Compared to animals in which oligodendrocyte development was unperturbed, animals subjected to postnatal oligodendrocyte loss showed delayed recovery from an LPC lesion to the mature spinal cord. Unexpectedly, the induction and severity of MOG induced EAE was not significantly altered in animals following oligodendrocyte developmental loss even though there was a substantial increase in spinal cord tissue damage and CNS inflammation. It is unclear why the elevated glial responses seen in developmentally compromised animals were not reflected in enhanced functional deficits. These observations suggest that developmental loss of oligodendrocytes results in long lasting tissue changes that alter its response to subsequent insults and the capacity for repair in the adult.

1. Introduction

The central nervous system (CNS) demyelinating disease Multiple Sclerosis (MS) is characterized by oligodendrocyte loss, focal demyelination, microglial activation, immune cell infiltration, and inflammation that is correlated with functional deficits. The causes of MS are unclear and a variety of risk factors including gender, genetics, vitamin D deficiency, race and certain viral infections have been associated with enhanced susceptibility to MS (Kamel, 2019). Insults to the CNS may also initiate CNS demyelination directly or indirectly. For example, oligodendrocyte ablation studies in adult mice demonstrate that animals that survive the initial loss of oligodendrocytes and undergo remyelination are susceptible to subsequent attacks (Traka et al., 2016) although whether this represents anti-CNS immunity is unclear (Locatelli et al., 2012). Epidemiological studies, however indicate that environmental factors early in life influence the prevalence and development of adult disease (Gluckman et al., 2008) suggesting a lasting effect of early events. The concept that early insults influence the progression of adult disease is not restricted to MS and has been proposed for a number of diseases including Crohn's disease (Sonnenberg and Ajdacic-Gross, 2018), asthma (Eagleton et al., 2002), and autism (Dietert et al., 2011), where exposure to an insult such as infectious agents early in development has a persistent influence on the neuroimmune responses (Boisse et al., 2004) and cognitive functions that becomes apparent following a second challenge or insult to the adult CNS (Bilbo et al., 2005; Cunningham et al., 2009). Mechanistically, it has been proposed that this represents a priming

* Corresponding author.
E-mail address: ahdeah@gwu.edu (A. Pajoohesh-Ganji).

https://doi.org/10.1016/j.bbih.2020.100110
Received 14 July 2020; Accepted 19 July 2020
Available online 26 July 2020

phenomenon reflecting phenotypic alterations in the CNS microglial population characterized by increases in interleukin-1 beta (IL-1β) production (Hanamsagar and Bilbo, 2017). It is likely however, that priming of the CNS following developmental insults also involves other cell types and occurs in response to a broad range of perturbations other than infections.

We have previously utilized a transgenic mouse model (MBP-iCP9) that expresses an inducible form of caspase 9 (iCP9) driven by a fragment of the MBP promoter to locally target apoptosis in approximately 70% of mature oligodendrocytes (Caprariello et al., 2012, 2015) during development. Crosslinking iCP9, through local delivery of a chemical inducer of dimerization (CID), results in activation of the caspase pathway and the induction of apoptosis in MBP + mature oligodendrocytes without directly affecting other CNS cell types (Pajoohesh-Ganji and Miller, 2016, 2019). Loss of oligodendrocytes is assessed by loss of DsRed + cells, a reporter linked to iCP9 and driven off the same MBP promoter. These previous studies utilized a local injection of CID in the same area as the subsequent focal demyelination, potentially complicating the interpretation of the data and not allowing for systemic studies. In the present study, we have utilized a subcutaneous delivery of CID followed by either a focal spinal cord demyelinating lesion induced by lysophosphatidylcholine (LPC, lysolecithin) or the induction of experimental autoimmune encephalomyelitis (EAE) in adults. This approach allowed us to distinguish between priming due to loss of oligodendrocytes and secondary responses to early injections and to examine the effect of early oligodendrocyte loss on the onset and progression of EAE. We show that while early ablation of oligodendrocytes results in a reduction in myelin and functional deficits, these recover relatively rapidly. Developmental loss of mature oligodendrocytes does, however, significantly impair recovery from an LPC lesion and increases CNS immunoreactivity in mature animals with EAE induced damage. Together these studies support the notion that perturbation of the oligodendrocyte lineages early in development enhances the susceptibility and reduces recovery from demyelinating insults to the adult CNS.

2. Methods

Animals and *in vivo* injections. All the studies comply with the George Washington University Medical Center Institutional Animal Care and Use Committee guidelines. Throughout this study, a combination of both male and female MBP-iCP9 transgenic mice (Caprariello et al., 2012) on a C57Black6 background were used for behavioral studies and lysolecithin injections. However, due to the limited number of transgenic animals, gender specific studies were not performed although no obvious gender differences were detected. For EAE induction studies, only female mice were used in accordance with standard protocols and the manufacturer's instruction.

Pups were injected subcutaneously starting on postnatal day 4 with 100 mg/Kg body weight of CID (clontech laboratories; #635069) daily for 7 days or every other day for a total of 7 injections. Stock solution of CID was made in 100% ethanol and diluted in equal volume of Polyethylene Glycol (PEG400, Fisher Scientific; #P167) and 1% Tween-20 in PBS. Controls were injected with vehicle (VEH) lacking CID, where 100% ethanol was added to PEG400 and 1% Tween-20 in PBS. Under terminal sedation, mice were sacrificed 2 weeks after the LPC and 2 or 4 weeks after the EAE studies and transcardially perfused with 1xPBS followed by fixative. Animals were fixed with either 4% paraformaldehyde (PFA) for immunefluorescence (IF) and histological staining or 4% paraformaldehyde + 2% glutaraldehyde in 0.1 M sodium cacodylate (PFA/GA) for Scanning Electron Microscopy (SEM). For immunoblotting, spinal cord tissues were snap-frozen in liquid nitrogen and stored at −80 °C.

LPC surgeries. Postnatal MBP-iCP9 transgenic mice were injected with VEH (n = 6) or CID (n = 11) as outlined above and allowed to mature to 6–7 weeks of age when a spinal cord LPC lesion was performed as previously described (Caprariello et al., 2015). Briefly, under isoflurane anesthesia, a small incision was made to expose the spinal cord between T11 and T12. A microinjector was used to administer 1 μl of 1% LPC (Sigma Aldridge) in 0.9% saline at a depth of 0.3 mm into the dorsal column of spinal cord over a period of 5 minuntes. After the injection was complete, the needle was left in place for an additional 2 minuntes to prevent fluid reflux. After suturing the skin, the animals were placed on a heating pad to recover before returning to the animal facility. Fourteen days post lesion (dpl) animals were sacrificed for histological staining (VEH n = 3, CID n = 6) or SEM analysis (VEH n = 3, CID n = 5).

Table 1
Mouse EAE scoring.

Score	Clinical observations
0	Not different than non-immunized mouse. Tail has tension and is erect. Hind legs spread apart.
0.5	Tip of tail is limp. The tail has tension except for the tip. Muscle straining is felt on the tail, while tail continues to move.
1	Limp tail. When picked up, tail drapes over finger. Hind legs spread apart. No signs of tail movement.
1.5	Limp tail and hind leg inhibition (one leg falls through wire rack). Walking is slightly wobbly.
2	Limp tail and weakness of hind legs. Legs not spread apart. Apparent wobbly walk. Toe dragging in one foot. *OR* head tilting. Poor balance
2.5	Limp tail and dragging of hind legs. Both hind legs have movement but mouse trips on hind feet. *OR* no movement in one leg/completely drags one leg, but movement in other leg. *OR* EAE severity is mild but a strong head tilt that causes the mouse to occasionally fall over.
3	Limp tail and complete paralysis of hind legs. *OR* one or both hind legs are able to paddle but not able to move forward. *OR* almost complete paralysis of hind legs. Limp tail and paralysis of one front and one hind leg. *OR* severe head tilting, walking at the end of the cage, pushing against the cage wall, spinning when pick up at the base of the tail.
3.5	Limp tail and complete paralysis of hind legs. Mouse moving but when place on its side unable to right itself. Hind legs are together on one side of the body. *OR* Mouse moving but the hind quarters are flat like a pancake, giving the appearance of a hump in the front quarters of the mouse.
4	Limp tail. Complete hind leg and partial front leg paralysis. Mouse not moving much but appears alert and feeding. Euthanasia is recommended if mouse scores 4 for 2 consecutive days. With daily saline injection mouse may recover to 3.5 or 3.
4.5	Complete hind leg and partial front leg paralysis. No movement. Mouse is not alert and barely responds to contact. Euthanasia is recommended.
5	Mouse is spontaneously rolling in the cage. Mouse is dead or euthanized due to severe paralysis.

EAE induction. Female VEH (n = 10) or CID (n = 12) injected animals were allowed to mature to 10–11 weeks and induced with EAE using MOG_{35-55} peptide according to the manufacturer's guidelines (Hooke Laboratories #EK-2110). Briefly, animals were injected with MOG_{35-55} emulsion and pertussis toxin on day 0 and again with a second dose of pertussis toxin on day 1. Animals showed symptoms of EAE approximately 8 days after induction and were scored on a daily basis according to the following criteria: 1 loss of tail tonicity or hind limb weakness to 5 severe paralysis or death (Table 1). Animals scored 3 or higher were given 0.2 ml saline daily to prevent dehydration. Animals were sacrificed for histological or ultrastructural analysis at 2 weeks (VEH n = 2, CID n = 2) or 4 weeks (VEH n = 8, CID n = 10). All investigators were blinded to the animal treatments when performing the behavioral studies.

Open field testing. For functional testing, mice were placed in a Plexiglass open field (Med Associates, St Albans, VT, USA) outfitted with photobeam detectors, and their activities were monitored using the activity monitoring software (Med Associates). Mice (CID n = 5 and VEH n = 3) were allowed to habituate in the open field for 10 min and the total distance traveled and speed were recorded at 21 and 28 days postnatally (Polter et al., 2010). Duration of open field was kept constant among all mice and for both time-points.

Tissue processing. Tissues were processed for 3 different analyses. 1)

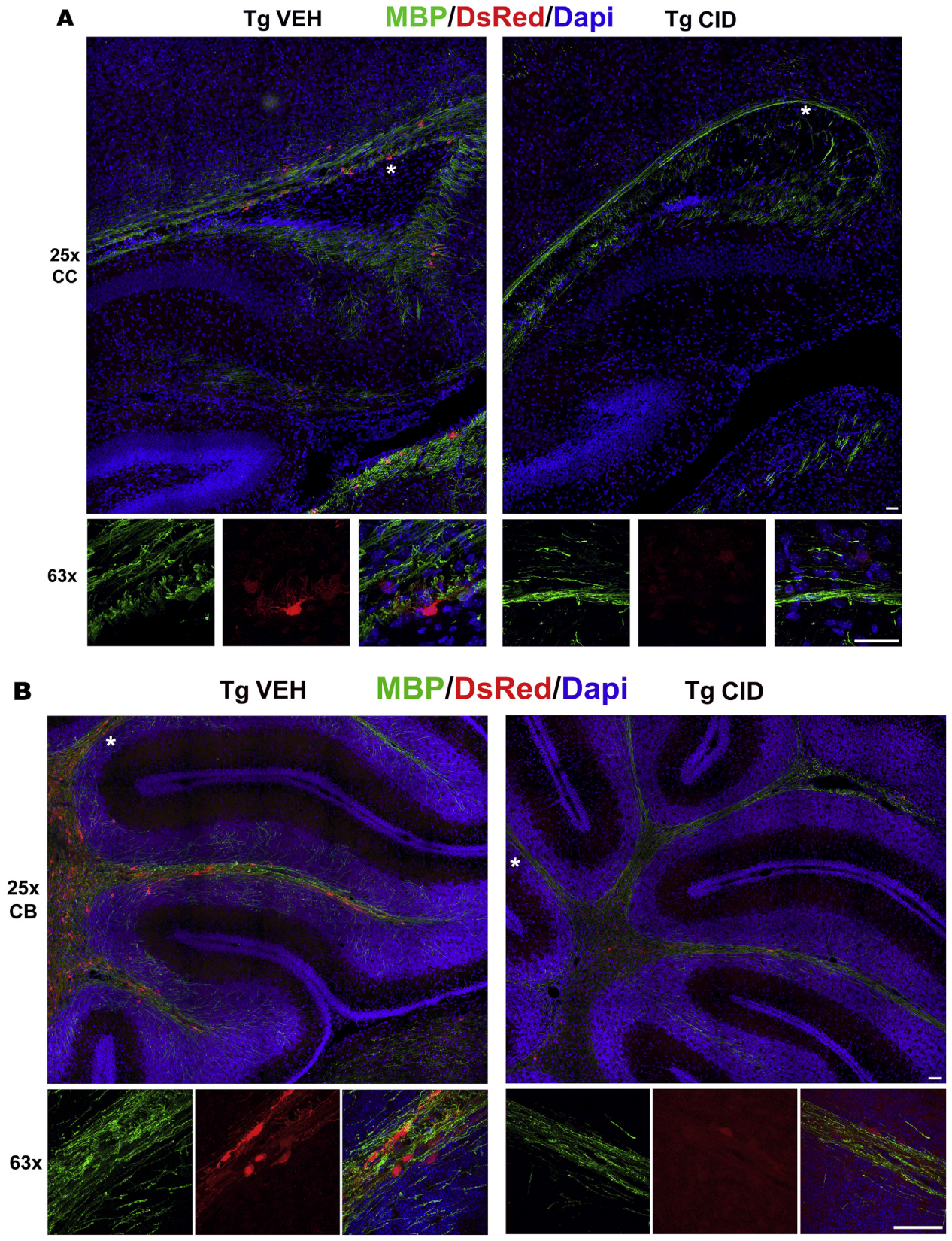

Fig. 1. Systemic CID injection induces loss of DsRed + oligodendrocytes and a decrease in MBP staining throughout the CNS. Sections of tissues taken 3 days after the final injection of CID (P4–P11) show reduction in the number of oligodendrocytes and myelin throughout the CNS. Corpus callosum (**A**), cerebellum (**B**), optic nerve (**C**), and spinal cord (**D**) representative sections from MBP-iCP9 transgenic mice subcutaneously injected with vehicle (VEH) or CID (n = 3/group) were labeled with antibodies to MBP (green), DsRed (red), and DAPI (blue). The bottom panel in each image shows the areas indicated with an asterisk in the top panel (Bar = 25 μm). (For interpretation of the references to colour in this figure legend, the reader is referred to the Web version of this article.)

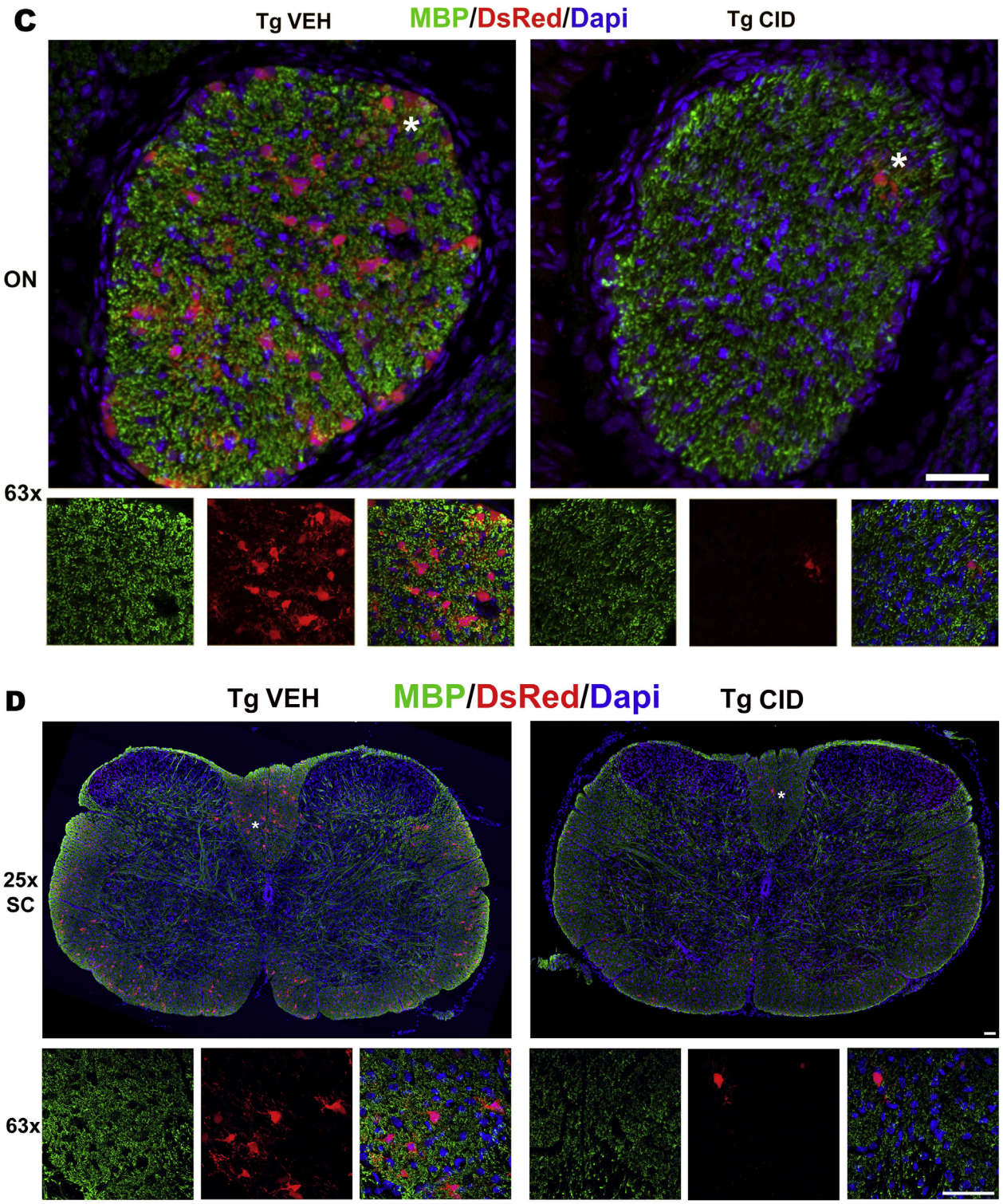

Fig. 1. (*continued*).

Immunofluorescence and histological staining: animals were fixed with PFA and spinal cords were cryoprotected using 10, 20, and 30% sucrose gradient in 1xPBS solutions; sections were cut at 20 μm. 2) *Electron Microscopy*: animals were fixed with PFA + GA and spinal cords were cut to 400 μm slices before processing. Slices were osmicated (1% OsO_4) for at least 4 h followed by incubation in 1% uranyl acetate overnight. After graded dehydration with ethanol and propylene oxide, samples were placed in Epon812 and sectioned at 1 μm or 120 nm using an ultramicrotome (Leica UC6). Sections were stained with Solochrome or Toluidine Blue to visualize myelin or placed on semiconductor grade Si-wafer microtome stubs for ultrastructural analysis. 3) *Immunoblotting*: animals were perfused with cold 1xPBS and spinal cords flash-frozen in liquid nitrogen and stored at −80 °C.

Immunostaining. Frozen sections were rehydrated, blocked, and incubated with primary antibodies overnight followed by appropriate secondary antibodies for an hour prior to mounting. The following primary antibodies were used: MBP (1:300- Abcam; #7349), DsRed (1:400- Takara; #632496), Iba1 (1:500- WACO; #019–19741), and GFAP

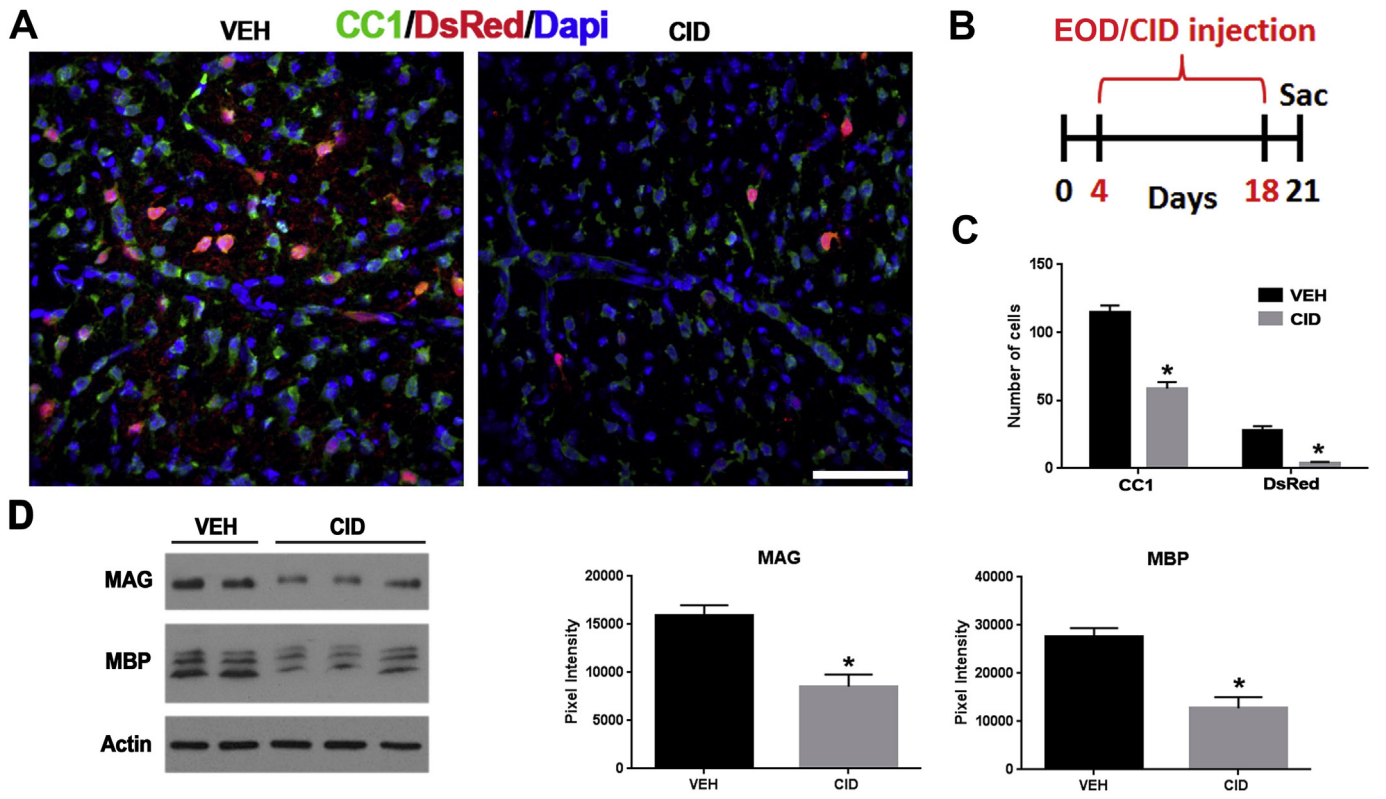

Fig. 2. Oligodendrocyte ablation results in a significant decrease in mature oligodendrocytes and a decrease in myelin proteins. A. Representative images of spinal cord sections labeled with antibodies to CC1 (green), DsRed (red), and DAPI (blue) in vehicle (VEH) and CID injected pups. Note that the CID injected animals (n = 2) show a significant decrease in CC1 and DsRed staining as compared to vehicle. **B.** Schematic of the every other day (EOD) CID injection and tissue collection. **C.** Quantification of cell numbers indicate a significant decrease in the number of mature CC1+ oligodendrocytes (p-value = 0.0312) and DsRed + cells (p-value = 0.0001) in CID injected, compared to VEH injected animals. CC1+ and DsRed + cells were counted from 6 areas (2 dorsal, 2 ventral, and 2 lateral) of the spinal cord. **D.** Western blot analysis of spinal cord tissue indicates that the myelin proteins MAG (p-value = 0.007) and MBP (p-value = 0.005) were decreased significantly after CID injection compared to VEH treated animals (CID n = 3 and VEH n = 2) (Bar = 25 μm). (For interpretation of the references to colour in this figure legend, the reader is referred to the Web version of this article.)

(1:500- Biolegend; #PRB-571C), PDGFαR (1:100- BD Biosciences; #558774), and CC1 (1:200- Millipore; #OP80). Appropriate secondary Alexa 488 or 594 (1:500) antibodies were used. Sections were counterstained with Dapi (1:1000- Thermofisher; #46190) before mounting (Fluoromount G: Electron Microscopy Sciences; #17984-25).

Immunoblotting. Frozen tissues were processed and lysates were run on 4–20% gels (BioRad; #456–1094). The following primary antibodies were used: MAG (1:5000, Generous gift from Dr. Richard H. Quarles (2007)), MBP (1:1000 for WB; Abcam; #7349), and Actin (1:2000; Santa Cruz; #SC47778) antibodies. Appropriate secondary antibodies were used at 1:5000.

Microscopy. Microscopy was performed at the Center for Microscopy and Image Analysis (CMIA) at the George Washington University Medical Center. Confocal microscopy images were captured using the Zeiss Cell Observer Z1 spinning disk confocal microscope (Carl Zeiss, Inc.) equipped with ASIMS-2000 (applied scientific Instrumentation) scanning stage with z-galvo motor, and Yokogawa CSU-X1 spinning disk. Zen Blue software (Carl Zeiss, Inc.) was used with 25x and 63x objectives to acquire tile images and produce maximum intensity projections. SEM was performed using a Helios NanoLab 660 SEM (Thermo Fisher, FEI) equipped with a concentric backscattering detector (CBS) using immersion mode for SEM high-resolution imaging. Acquisition conditions included 2 kV with a landing current ranging from 0.2-0.4 nA and a working distance of 4 mm. For imaging, the entire spinal cord was tile-imaged at low magnification (600×) and fused into a single tiling map per sample and used as a navigation map to identify lesioned areas (MAPS software). Then, high-resolution (3,500x or 15,000x) imaging was performed in the focus area at 10 ms dwell time and 20 mm horizontal field of view.

Statistical Analyses. All statistical tests were performed using the GraphPad Prism Program, Version 6 (GraphPad Software, Inc. San Diego, CA). A p value <0.05 was considered statistically significant and is demarked with an asterisk. NIH Image J was used to analyze and quantify pixel intensity for Western blot and immunofluorescent analyses (Figs. 2 and 3) followed by Student's t-test to assess significant differences in mean band intensity between VEH and CID treated samples. Photoshop was used to calculate the area of the lesion (Fig. 5) and quantify cells and remyelinated axons in 3 random sites (n = 5 CID and n = 3 VEH) of the spinal cord (Fig. 6). Significance of the differences between the numbers of remyelinated axons in VEH and CID treated samples was determined using Student's t-test.

To quantify GFAP and Iba1 staining in EAE animals (Figs. 8 and 9), eight areas (2 dorsal, 2 ventral, 2 lateral, 1 mid-ventral, and 1 central) from each section in 2 different animals were analyzed. A depiction of the areas is provided in the figures. Student's t-test was utilized to determine if the means of pixel intensity was different between VEH and CID treated tissues.

3. Results

3.1. Systemic injection of CID ablates oligodendrocytes throughout the CNS

In previous studies, local injections of CID into MBP-iCP9 transgenic (TG) mice have been used to specifically ablate a proportion of oligodendrocytes locally in regions of the spinal cord (Caprariello et al., 2015),

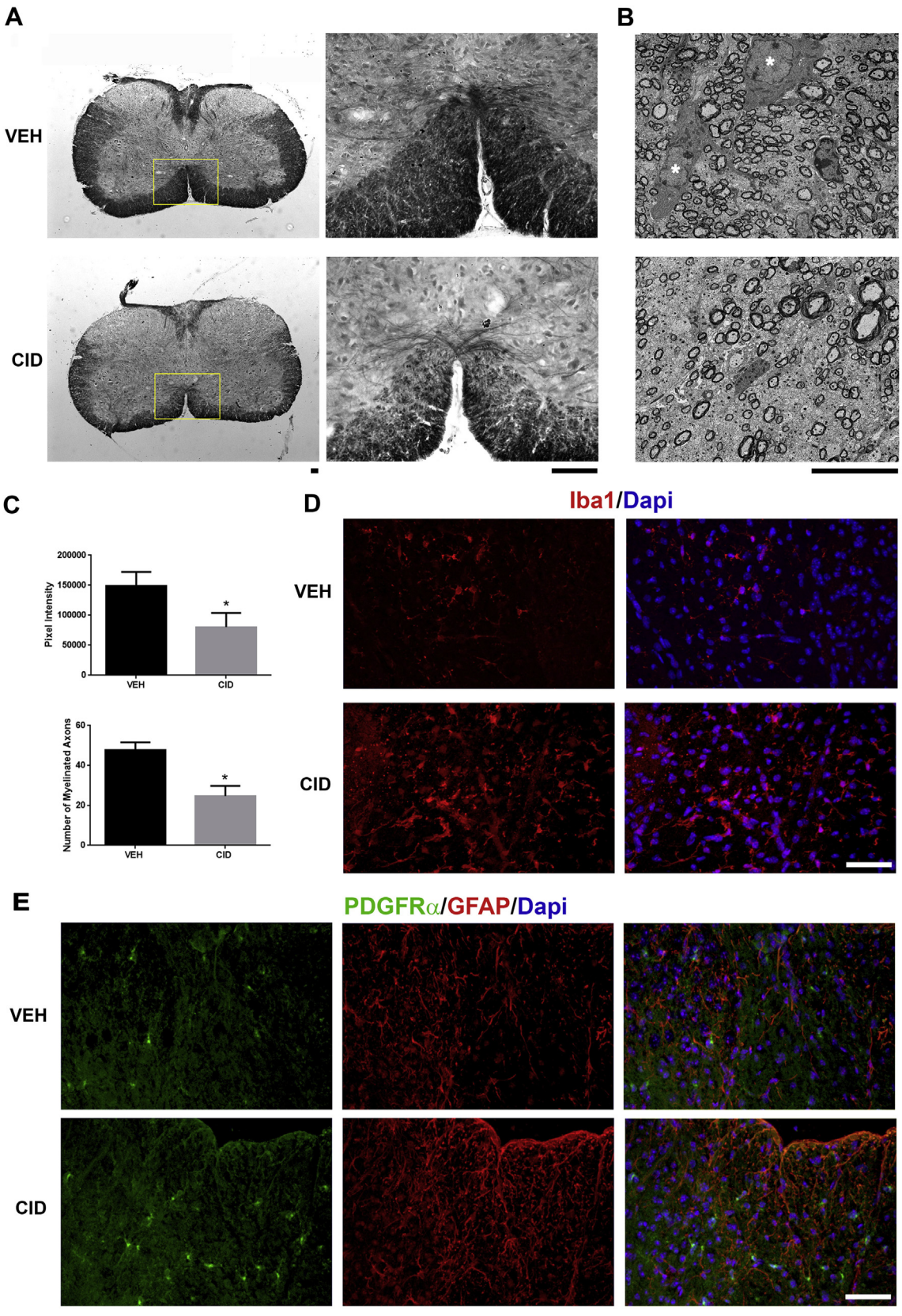

(caption on next page)

Fig. 3. Developmental ablation of mature oligodendrocytes results in a decrease in myelinated axons, an increase in astrocytes and microglial activation, and elevated numbers of oligodendrocyte progenitor cells. A. Representative images of spinal cord sections stained with Solochrome indicate a decrease in myelin staining observed throughout the white matter in animals treated with CID (n = 3) compared to vehicle (VEH) treated controls (n = 2). Yellow boxes represent magnified areas. **B.** Ultrastructural analyses confirmed the decrease in myelinated axons in CID compared to VEH treated spinal cord. Healthy oligodendrocytes (white asterisk) are apparent in the VEH image associated with neighboring axons. **C.** Quantification of Solochrome images (top graph) and EM sections (bottom graph) show significant decrease in levels of myelin and the number of myelinated axons in CID compared to VEH animals. **D, E.** Oligodendrocyte ablation results in changes in adjacent glial cell populations. Sections from spinal cord injected with VEH or CID were labeled with antibodies to Iba1 (red in **D**), PDGFRα (green in **E**), GFAP (red in **E**), and Dapi (blue). CID treated animals demonstrated increased Iba1 (D) and GFAP (E) immunoreactive and higher number of OPCs compared to VEH animals. (Bar = 10 μm in A and B, Bar = 25 μm in D and E). (For interpretation of the references to colour in this figure legend, the reader is referred to the Web version of this article.)

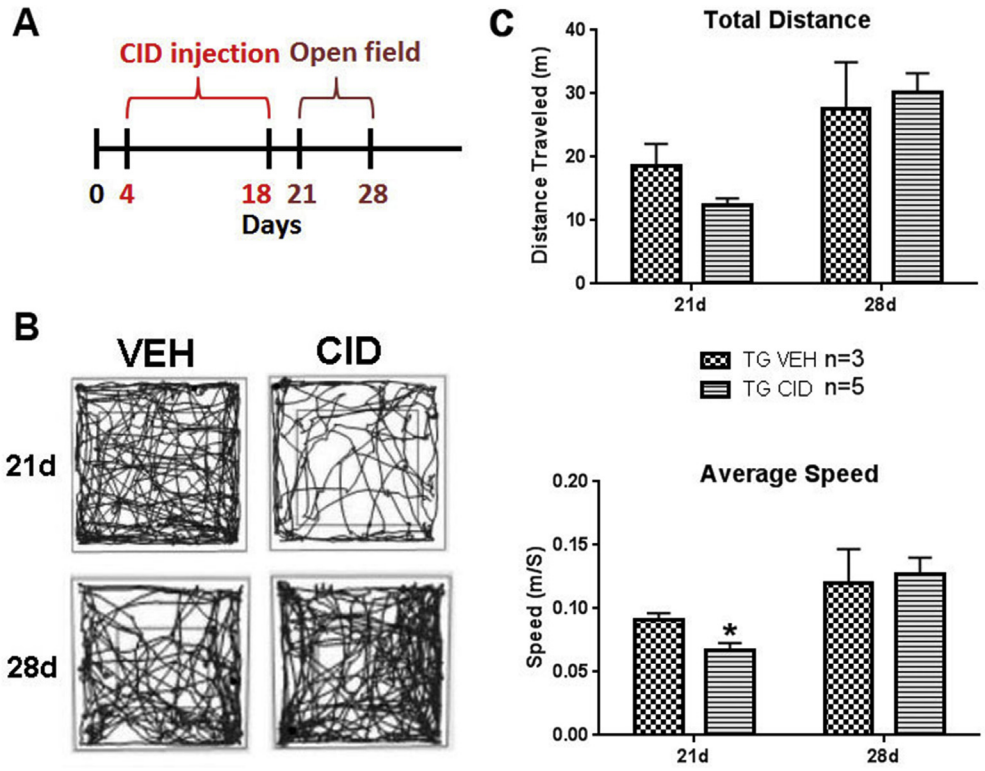

Fig. 4. Oligodendrocytes ablation results in a transient functional deficit. A. Schematic of the CID injection and open filed testing. **B.** Representative traces obtained from mice at P21 (3 days post-CID) and P28 (10 days post-CID) (vehicle/VEH n = 3, CID n = 5). At P21, the motility of the animals is significantly reduced in CID treated animals compared to VEH treated controls as indicated by the density of traces. At P28 the level of motility between the two groups was similar. **C.** Quantification of the differences in total distance and average speed traveled indicates a decrease in total distance and a significant decrease (p-value = 0.0316) in average speed traveled by CID treated mice at 3 days post-CID (21 days) that was resolved by10 days post-CID (28 days).

which ultimately recovers, and in the optic nerve (Pajoohesh-Ganji and Miller, 2016, 2019), where recovery is delayed. In the current study we assessed the effects of systemic loss of oligodendrocytes during development on myelination and on recovery in response to adult demyelinating insults. Systemic, subcutaneous-injection of CID into MBP-iCP9 animals (n = 3) for 7 consecutive days, starting 4 days after birth, results in decrease in the density of mature oligodendrocytes 3 days after the final injection as detected by DsRed labeling in different areas of the brain including the corpus callosum and cerebellum (Fig. 1A and B), the optic nerve (Fig. 1C), and the spinal cord (Fig. 1D) while TG controls (n = 3) were unaffected by vehicle injections. Similar levels of oligodendrocyte loss were seen in MBP-iCP9 animals that received every other day (EOD) CID injections (n = 2) and all subsequent studies were performed on animals receiving alternate daily injections (Fig. 2A and B). Myelin perturbation in oligodendrocyte ablated mice resulted in reduced MBP staining throughout the CNS (Fig. 1) and a significant decrease in the level of the myelin proteins MAG (p-value = 0.007) and MBP (p-value = 0.005) in spinal cord tissues (Fig. 2D). No obvious regional differences were seen in the loss of oligodendrocytes in response to systemic CID delivery. All regions of the CNS showed reductions in myelin intensity (Fig. 1) and an approximately 50% reduction in the number of CC1+ oligodendrocytes after CID injections (Fig. 2A and C).

3.2. Systemic ablation of mature oligodendrocytes during development leads to myelin loss, glial activation, and transient functional deficits

To further analyze the effect of oligodendrocyte ablation on myelin formation, spinal cord sections from CID injected and control animals were stained with Solochrome 3 days after the final injection (Fig. 3A) and the relative intensity assayed. Following CID injections (n = 3), a significant reduction (p-value = 0.0004) in the level of Solochrome staining was apparent (Fig. 3C), particularly in the ventral spinal cord (Fig. 3A), suggesting a reduction in myelination. Consistent with these observations, ultrastructural analysis showed a significant reduction (p-value = 0.0001) in the number of myelinated axons (Fig. 3B and C) at P21 in ten different regions of the ventral spinal cord. While VEH treated animals had on average density of 48/100 μm^2 myelinated axons, in CID treated animals this was reduced to 26/100 μm^2. In general, the myelin present in CID treated animals appeared relatively normal and there were no significant differences in the G ratios. The loss of mature oligodendrocyte affected other glial populations. Three days after CID delivery, astrocytes were activated as indicated by an increase in GFAP + processes (Fig. 3E), while microglial morphology changed from ramified to amoeboid and an increase in Iba1 was observed suggesting their activation (Fig. 3D). In addition, the number of PDGFRα+ oligodendrocyte progenitor cells (OPCs) was also increased following ablation of mature oligodendrocytes (Fig. 3E).

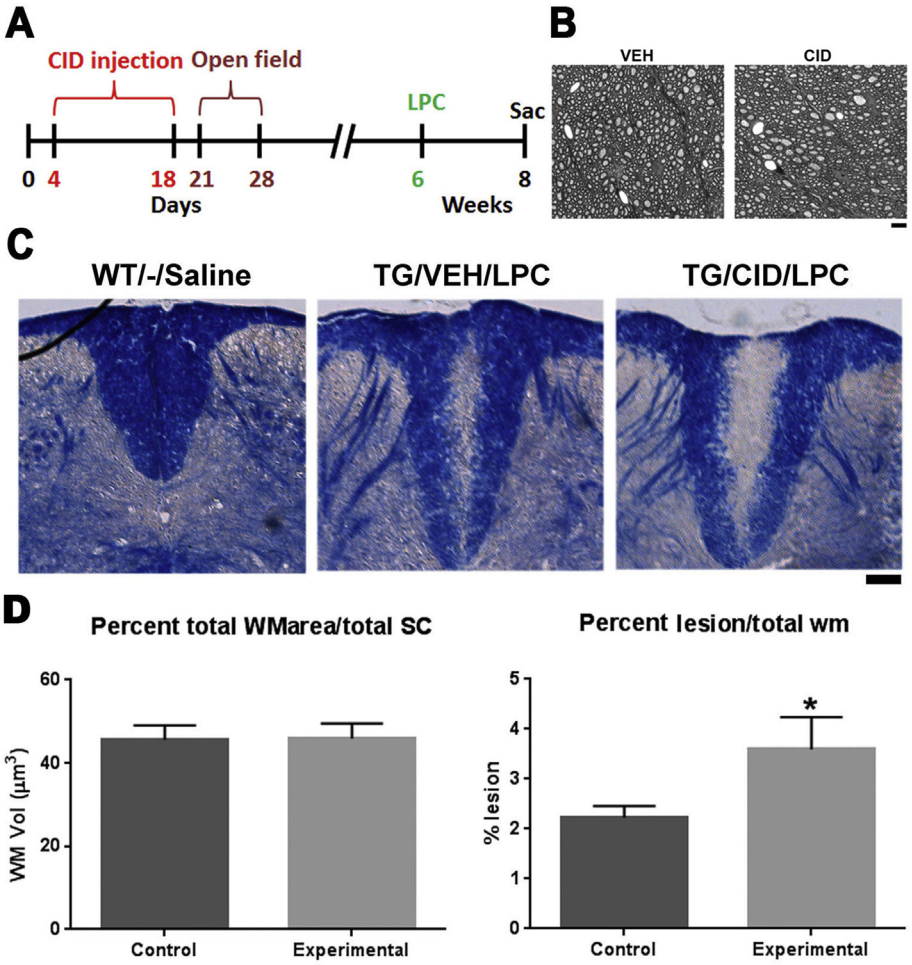

Fig. 5. Larger LPC-induced demyelinated lesions are present in CID treated mice than controls. A. Schematic of the CID injection and the time-line for LPC injections. **B.** Representative EM images from the ventral regions show no significant differences in the number of myelinated axons and myelin thickness between VEH and CID treated animals at 8 weeks of age. **C.** Representative images show sections from wild type (WT) mouse injected with saline (WT/-/Saline), MBP-iCP9 transgenic mouse injected with vehicle (VEH) followed by LPC (TG/VEH/LPC), and MBP-iCP9 transgenic mouse injected with CID followed by LPC (TG/CID/LPC). Sections were taken 14 days after LPC injection. WT mice injected with saline did not show any detectable lesion. WT/CID/LPC and TG/VEH/LPC treated mice (Controls) served as control groups in which oligodendrocytes were not ablated. **D.** The total volume of white matter (WM) area was compared to the total volume of spinal cord across all groups and no significant differences were detected suggesting that normal myelination was unaffected by creation of the transgenic phenotype. Two sections from each animal were assessed and the relative proportion of lesioned dorsal white matter was significantly (p-value = 0.0039) higher in experimental transgenic mice, that had received CID and LPC (n = 3) compared to those that received vehicle and LPC or wild type mice that received CID (n = 2) suggesting slower remyelination in the CID treated transgenic mice (Bar in B = 25 µm).

The reduction in oligodendrocytes results in transient functional deficits. Following developmental ablation of mature oligodendrocytes between P4–P18, animals showed reduced mobility at P21 that had largely recovered one week later at P28 (Fig. 4). In open field studies, animals subjected to oligodendrocyte ablation showed a reduction in the total distance traveled compared to VEH injected controls at P21 (Fig. 4B and C). The average speed of movement was also significantly reduced (p-value = 0.0316) in animals following oligodendrocyte ablation compared to VEH treated controls (Fig. 4C). The changes in motility were transient and no significant differences between experimental and control animals were detected at P28. These data suggest oligodendrocyte ablation and reduction in CNS myelin impairs motor activity and that the functional recovery may reflect a normalization of CNS myelin.

3.3. *Developmental ablation of mature oligodendrocytes delays adult remyelination*

Previous studies suggested that local ablation of oligodendrocytes resulted in impaired repair following an adult demyelinating lesion (Caprariello et al., 2015). Interpretation of that data was, however complicated due to potential responses to the local injection of CID. In the current study, we have utilized subcutaneous systemic delivery of CID to eliminate this complication and facilitate EAE studies. The rate of remyelination following a spinal cord LPC lesion was compared in MBP-iCP9 TG animals that received CID injection against control (wild type mice injected with CID and TG mice injected with vehicle at 6 weeks of age) (Fig. 5A). Using EM sections, we compared the number of myelinated axons and their thickness in ventral regions that did not receive an LPC lesion at 8 weeks of age and did not observe any differences between VEH and CID sections (Fig. 5B). Injection of saline into wild type (WT/-/Saline) (Fig. 5C) or MBP-iCP9 animals showed no significant demyelination as previously reported (Caprariello et al., 2015). Comparison of the lesion area by Solochrome labeling 2 weeks after an LPC lesion demonstrated smaller residual lesions in control (n = 2) compared to experimental (n = 3) animals (Fig. 5C). To quantify the differences in lesion size, the relative proportion of affected dorsal spinal cord white matter was compared against total dorsal white matter area at 8 weeks of age. No differences in total dorsal white matter area were seen between control and CID injected animals (Fig. 5D). By contrast, at 14 days post-lesion (dpl) the proportion of lesion area was significantly different (p-value = 0.0039) between control and CID treated animals. The average lesion area constituted approximately 20% of dorsal white matter area in control and approximately 40% in CID treated animals suggesting that systemic depletion of oligodendrocytes during development inhibits adult myelin repair.

To directly assess remyelination, the morphology of lesions in VEH and CID treated animals were assessed by Toluidine blue staining and ultrastructural analyses at 14dpl. Remyelination was more evident in VEH treated animals (n = 3) and greatly reduced in CID treated animals. In VEH treated animals, profiles of thinly myelinated axons were distributed throughout the lesion particularly associated with blood vessels and the number of macrophage-like cells was relatively low. By contrast, ultrastructural analysis confirmed a significantly lower (p-value = 0.0225) number of thinly remyelinated axons in CID treated animals (n = 5) compared to VEH treated animals (Fig. 6) as well as a higher density phagocytic macrophage-like cells. Together this data is consistent with the proposal that adult remyelination in the LPC model is impaired by developmental loss of mature oligodendrocytes.

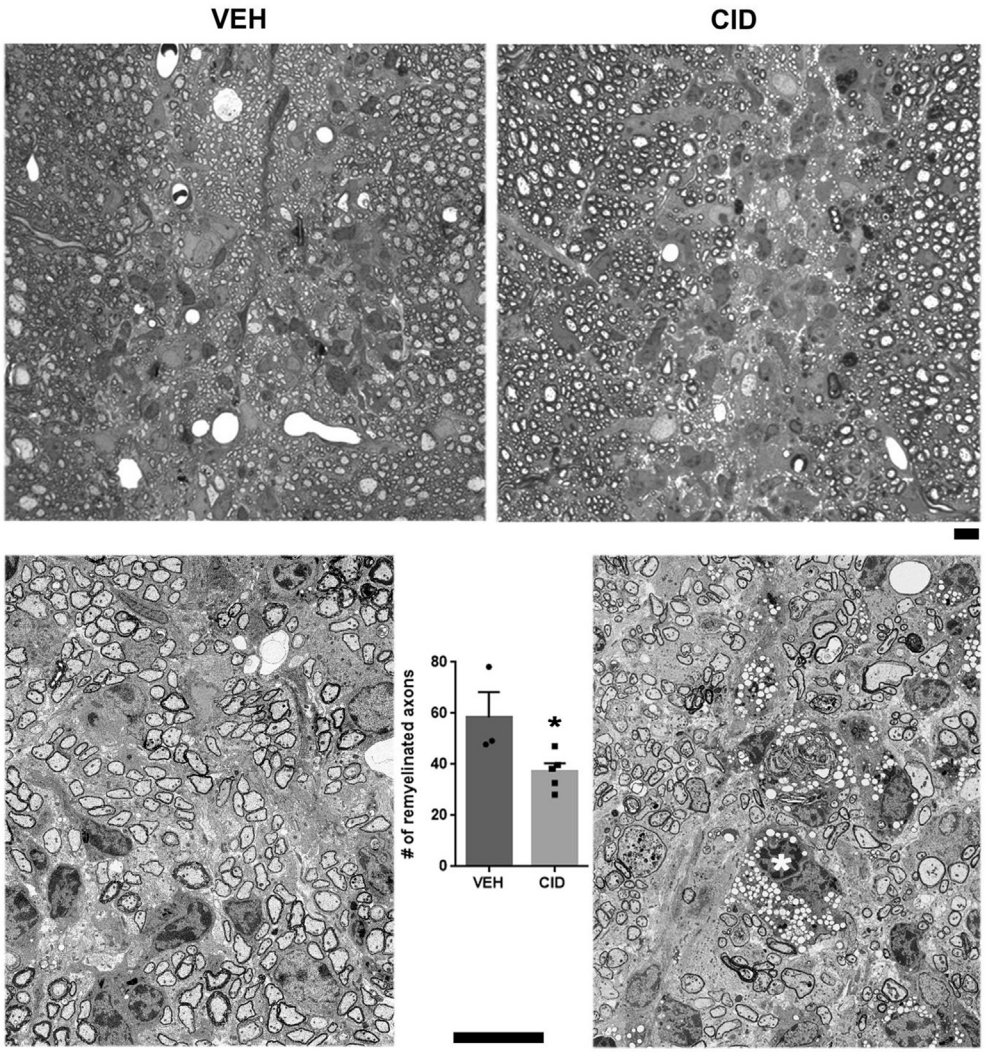

Fig. 6. Remyelination is reduced in LPC-induced demyelination in CID treated transgenic mice. Vehicle (VEH, n = 3) and CID treated (n = 5) MBP-iCP9 transgenic mice were injected with LPC at 6 weeks (about 4 weeks after the last CID injection) and sacrificed at 8 weeks of age. Sections were stained using Toluidine Blue stain (upper panels) and remyelinated axons were counted in three regions in the dorsal column. There is a significant decrease (p-value = 0.0225) in the number of remyelinated axons indicating decreased recovery in the CID treated mice. Lower panels show the SEM images. Note the lower level of myelinated axons and the presence of foamy macrophages in the CID treated tissue as indicated by the asterisk (Bar = 10 μm).

3.4. Developmental ablation of mature oligodendrocytes increases immune cell activation in EAE

Since developmental ablation of oligodendrocytes impaired remyelination in the LPC model, we examined its effects in the MOG_{35-55}-EAE animal model that results in both chronic and immunologically based demyelination. Female MBP-iCP9 animals that had received either VEH (n = 8) or CID (n = 9) injections during the P4–P18 developmental period were induced with EAE at 11 weeks of age and the development of the disease assayed for up to 28 days (Fig. 7A). Comparison of the clinical scores showed no significant differences in the timing of disease onset, the rate of increase in disease severity, or the final level of functional deficits between VEH and CID treated animals 4 weeks after EAE induction (Fig. 7B and C) suggesting that impairment of remyelination did not exacerbate disease progression. However, histological and cellular analysis of the spinal cord showed significant differences between EAE VEH and CID treated animals. Although the extent of EAE lesions vary throughout the spinal cord and are relatively diffuse, the lesions in CID treated animals appeared to be more severe and contained more degenerating axons with residual myelin sheaths that were less well compacted compared to controls (Fig. 7D). The levels of CNS inflammatory cell responses were significantly elevated in tissue from CID treated animals compared to VEH treated controls. For example, significant increases in the levels of astrocyte reactivity assayed by elevated expression of GFAP immunoreactivity were observed in CID treated animals at 2 (p-value = 0.0364) and 4 (p-value = 0.0003) weeks after EAE induction throughout the spinal cord (Fig. 8). Similarly, elevated levels of microglial activation assayed by elevated expression of Iba1 immunoreactivity and an increase in the development of amoeboid morphology were observed in CID treated animals at 2 (p-value = 0.0161) and 4 (p-value = 0.0001) weeks after EAE induction (Fig. 9). Together these data suggest that developmental loss of oligodendrocyte results in an elevated CNS immune response in the setting of adult onset EAE. Why such an increase in inflammatory response does not result in a worsening of the clinical score is currently unclear.

4. Discussion

Previous studies have utilized the MBP-iCP9 model to examine the mechanisms of cell death and the consequences of oligodendrocyte loss in the spinal cord and optic nerve (Caprariello et al., 2015; Pajoohesh-Ganji and Miller, 2016, 2019). These studies have largely relied on the focal injection of CID that results in a local area of demyelination. In the current study we expand these observations in 3 ways. First, we show that systemic delivery of CID through a subcutaneous injection results in widespread reduction of myelin and loss of oligodendrocytes. Second, the loss of approximately 50% of oligodendrocytes and myelin during postnatal development compromises animal mobility. Third, while adult remyelination is negatively affected by developmental mature oligodendrocyte loss as seen in the gliotoxin based LPC model, the functional

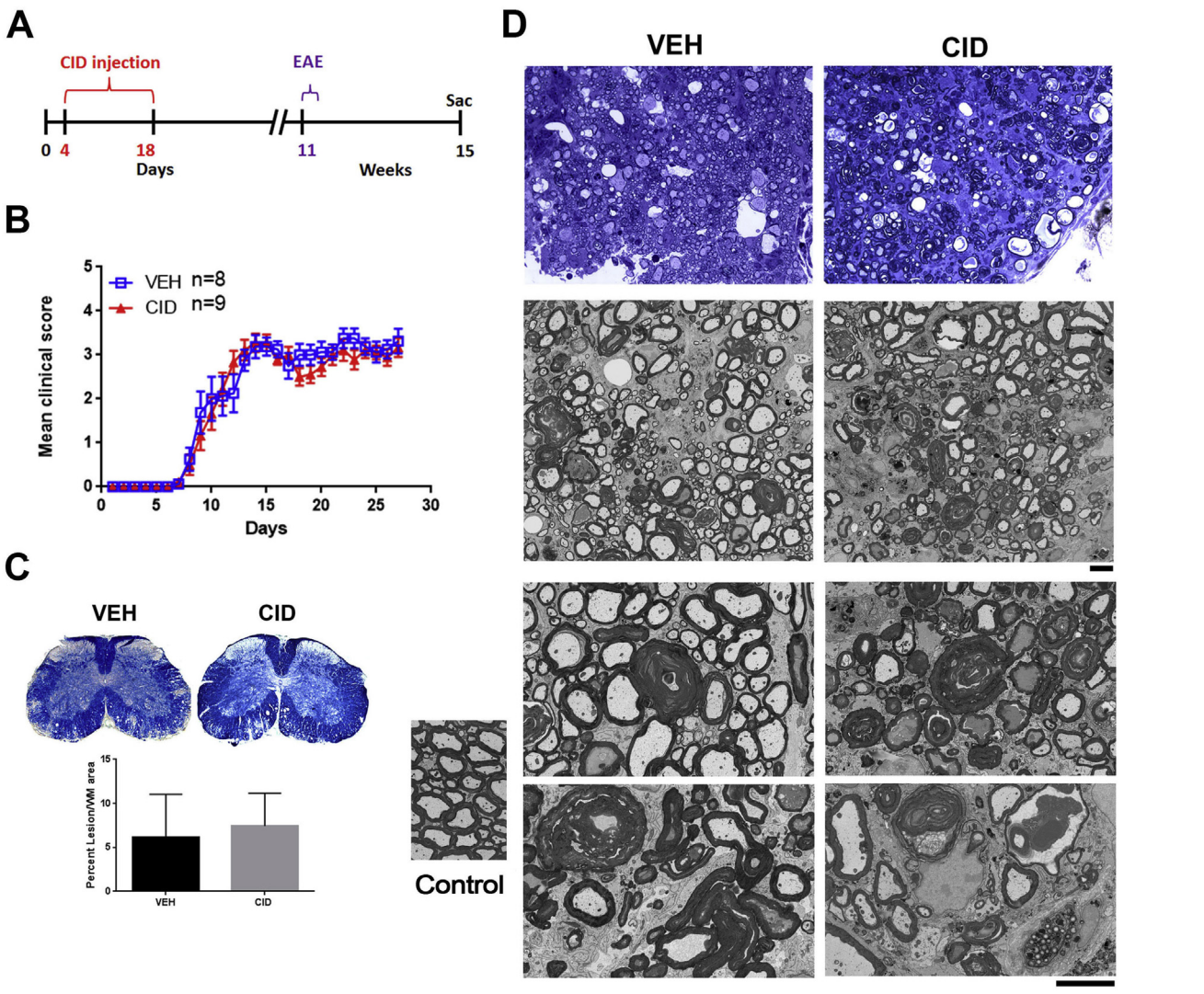

Fig. 7. CID treated animals have worse histological outcomes in EAE, which is not reflected in the functional outcome. A. Schematic of the CID injection and the timeline for EAE induction. **B.** Both Vehicle (VEH, n = 8) and CID (n = 9) treated mice were induced with EAE at 11 weeks of age (about 8 weeks after CID injection). There are no significant differences in the severity of the disease as indicated by the mean clinical score (**B**) or the overall level of lesion load based on Solochrome staining (**C**). However, the tissue integrity (**D**) was worse in the CID treated with a greater degree of myelin perturbation and axonal degeneration (Bar = 5 μm).

outcomes in the immune mediated model EAE appears unaffected even though CNS cellular immunoreactivity was elevated.

Apoptosis of oligodendrocytes during postnatal development has short-term and long-term impacts on CNS tissue. Exposure to CID in MBP-iCP9 animals results in the specific loss of mature oligodendrocytes through apoptosis (Caprariello et al., 2012), however the induction of cell death in oligodendrocytes has indirect effects on other neural cell populations. For example, CID induced-oligodendrocyte ablation results in an increase in PDGFRα+ OPCs in the spinal cord as well as activation of astrocytes reflected by an increased expression of GFAP immunoreactivity in their processes. The molecular basis of these changes is unclear. The increase in OPCs may reflect a negative feedback loop in which the loss of oligodendrocytes stimulates the production of OPCs. Such a regulatory system has been proposed for OPCs (Nakatsuji and Miller, 2001a, 2001b) and myelin is known to regulate OPC differentiation (Kotter et al., 2006; Robinson and Miller, 1999; Plemel et al., 2013; Syed et al., 2008). Cells undergoing apoptosis have been shown to express signals (eat me) including DAMPs (Kiernan et al., 2016), phosphatidylserine and lysophospatidylcholine that stimulate the phagocytic activity of nearby macrophages and microglia (Ravichandran, 2010; Tyurin et al., 2014; Mueller et al., 2007) and it seems likely that such signals may also be responsible for astrocyte activation. Consistent with this hypothesis, 3 days after the last CID treatment, Iba1+ microglia in the spinal cord developed an amoeboid morphology suggesting their activation. Whether the loss of oligodendrocytes/myelin or activation of the innate immune system is responsible for the changes in animal motility is currently unclear although patients with minimal symptoms of MS also show a decrease in gait velocity, due to poor stability and this increases with disease progression (Novotna, 2019). Although the most obvious effects of developmental loss of oligodendrocytes on CNS tissue are transient (namely the reduction in myelination), there are more subtle long-lasting effects. These are evident in the changes in myelin repair seen with LPC lesions and the enhanced inflammatory responses seen in EAE. Which cell population retains the memory of the first insult is unknown, but it is likely to be either astrocytes or microglia given their subsequent response to adult injury.

The concept that injuries, infection or other perturbations during postnatal development result in long-lasting changes in CNS immune cells has been proposed in other conditions. For instance, studies have shown that exposure to an insult such as an infectious agent early in

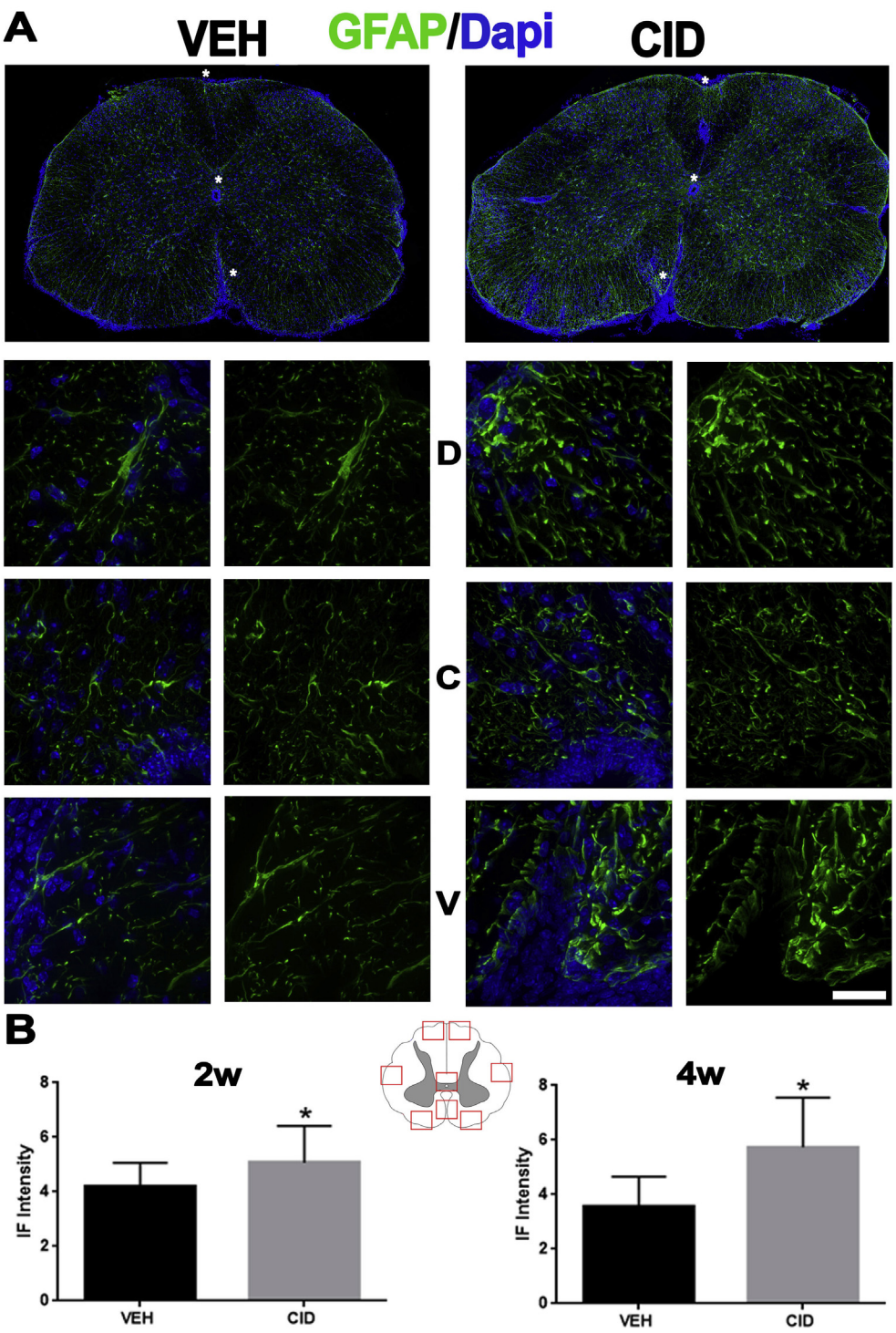

Fig. 8. Astrocyte activation is increased in the spinal cord of animals with EAE that were subjected to developmental ablation of mature oligodendrocytes. A. Sections from spinal cord of EAE mice treated developmentally with vehicle (VEH, n = 2) or CID (n = 2) were labeled with antibodies to GFAP (green) and Dapi (blue) 2 weeks after EAE induction. Bottom panels show higher magnifications (63×) of the areas indicated by asterisks in the lower magnification (25×) images in the top panels. The higher magnification areas are taken from (top to bottom) the dorsal (D), near the central canal (C), and ventral (V) spinal cord. **B.** Intensity of immunofluorescent staining was measured using image J in 8 different areas from each mouse, as depicted in the cartoon. Astrocytes are significantly more activated in the CID treated tissues at 2 (p-value = 0.0364) and 4 weeks (p-value = 0.0003) after EAE induction (Bar = 25 μm in **A**). (For interpretation of the references to colour in this figure legend, the reader is referred to the Web version of this article.)

development may influence neuroimmune responses (Boisse et al., 2004) and cognitive functions in adulthood that become evident upon a second challenge or insult (Bilbo et al., 2005; Cunningham et al., 2009). This appears to reflect a priming phenomenon in microglia that results in morphological changes and increased microglial IL-1β production (Hanamsagar and Bilbo, 2017). The initiation of priming is not restricted to infectious insults and may occur as a result of changes in the microenvironment involving multiple CNS cell types and not all the effects of priming require a second insult to become evident. Patients that suffer from traumatic brain injury may have long lasting changes in microglial cell functions (Witcher et al., 2015). Likewise, individuals subjected to concussion have an elevated level of microglial activation that leaves them susceptible to depression (Witcher et al., 2015; Fenn et al., 2014; Ogura et al., 1999). In the current studies, several factors associated with the early loss of oligodendrocytes might impair remyelination and the functions of microglia in the adult. For example, exposure to dying oligodendrocytes may prime local microglia to retain an activated state and in response to a second stimulus rapidly elevate the production of proinflammatory cytokines (Hanamsagar and Bilbo, 2017) that impair recovery. Alternatively, exposure of microglia to oligodendrocyte debris during postnatal development may blunt the capacity of the cells to clear related debris later in life, possibly through long lasting receptor down

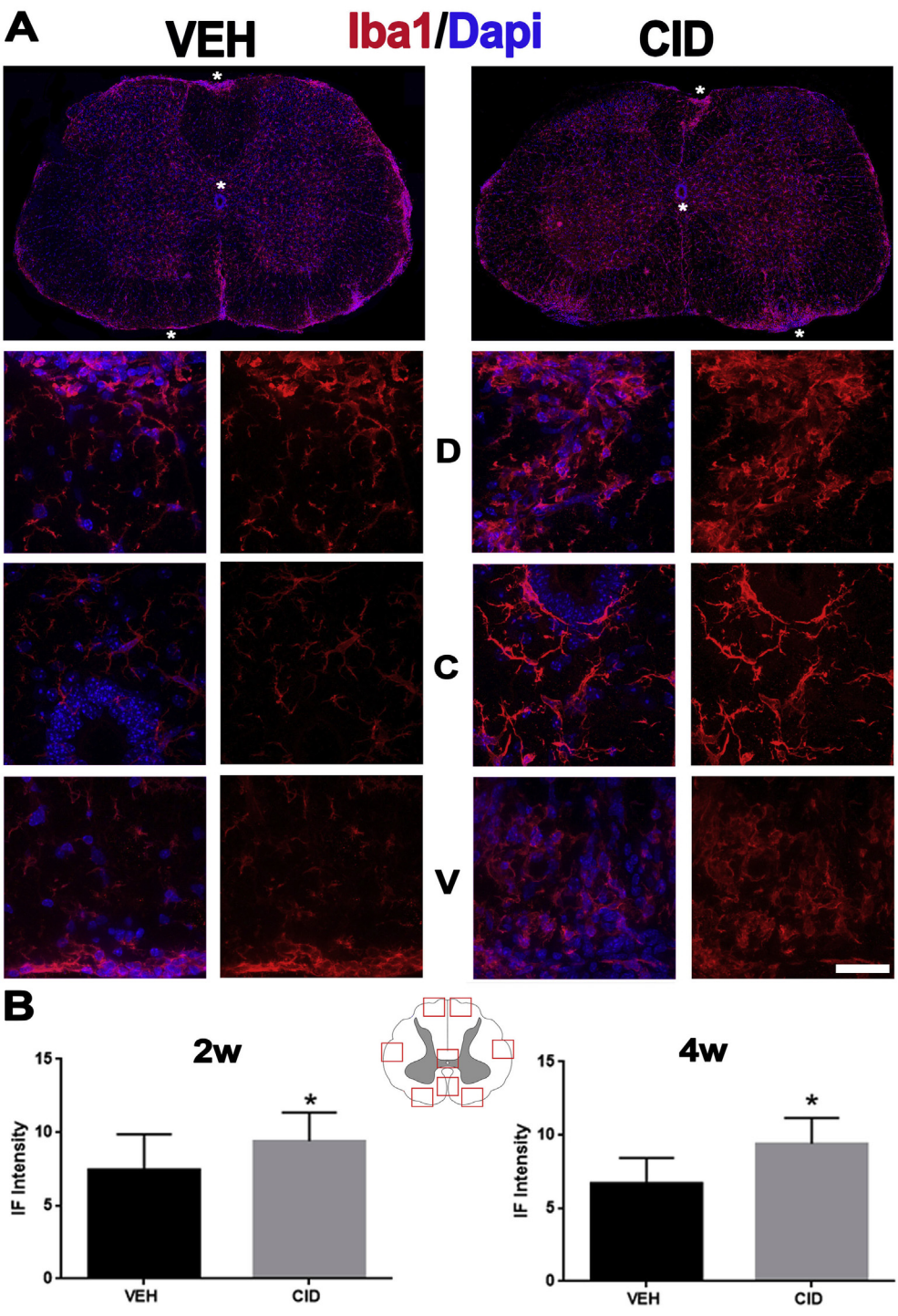

Fig. 9. Microglial activation is increased in the spinal cord of animals with EAE subjected to developmental ablation of mature oligodendrocytes. A. Sections from spinal cord of EAE mice treated with vehicle (VEH, n = 2) or CID (n = 2) were labeled with antibodies to Iba1 (red) and Dapi (blue) 2 weeks after EAE induction. Bottom panels show higher magnifications (63×) of the areas indicated by asterisks in the lower magnification (25×) images. The higher magnification areas are taken from (top to bottom) the dorsal (D), near the central canal (C), and ventral (V) spinal cord. The increase in the number and morphology of the microglia is evident in the CID treated tissues as indicated by the change in the staining intensity and the morphology of the microglia from more ramified in the VEH treated to more amoeboid in the CID treated tissues. **B.** Intensity of immunofluorescent staining was measured using image J in 8 different areas from each mouse, as depicted in the cartoon. Microglia are significantly more activated in the CID treated tissues at 2 (p-value = 0.0161) and 4 weeks (p-value = 0.0001) after EAE induction as indicated by increase in Iba1 labeling intensity and increased adoption of an amoeboid morphology (Bar = 25 μm in **A**). (For interpretation of the references to colour in this figure legend, the reader is referred to the Web version of this article.)

regulation or selective cell elimination. Such changes in microglia would result in an environment that was less conducive to repair. Indeed, the higher levels of myelin debris, axon damage, and inflammation in LPC and EAE CID treated animals strongly suggest environmental changes within the lesion that compromise repair.

One surprising observation from the current study was that although there was an increase in the levels of activated microglia and reactive astrocytes in EAE animals that had been subjected to developmental oligodendrocyte ablation, this did not appear to significantly alter the course of the disease. For instance, neither the timing of onset nor the peak level of disease were significantly altered in CID treated animals, which is inconsistent with the profound increases in immunoreactivity of astrocytes and microglia seen in the spinal cords of CID compared to VEH treated animals. While the basis for this discrepancy is unclear, it is possible that the functional deficits seen in the MOG_{35-55} model are not directly a reflection of spinal cord lesions but originate in other CNS regions. This seems highly unlikely given that in the MOG EAE model, the predominance of lesions are found in the spinal cord (Pierson et al., 2012; Lefeuvre, 2019). Alternatively, it may be that the majority of the functional deficits result from insults to selective axon tracks in the spinal cord and that additional insults to adjacent cord regions has little additive functional effects even though they are clearly evident histologically. Indeed unlike LPC lesions that have distinct borders, EAE produces diffuse lesions (McCarthy et al., 2012) that are more challenging to

quantify. It is also possible that the level of pathology induced by the MOG_{35-55} and pertussis toxin is sufficiently strong that the addition of a more repair-oriented insult resulting from developmental ablation of mature oligodendrocytes has no detectable impact on functionality. Decreasing the severity of EAE through use of a different model or reduction in the level of pertussis toxin stimulation may allow for the detection of incremental insults. Finally, in the EAE model the lack of repair may take an extended period of time to influence overall behavioral output and maintaining the animals for longer than 28 days post-EAE induction may reveal additional pathology. Further studies are required to clearly define the role of spinal cord inflammation in disease progression.

In conclusion, our data indicate that developmental ablation of mature oligodendrocytes induces short- and long-term changes in the CNS cellular environment. The short-term changes resolve within a few days but the long-term changes persist in a primed state for many weeks/months and become evident following perturbation of the adult CNS. The concept of developmental priming provides a possible explanation for the geographical linkage to increased susceptibility to MS established during childhood that becomes evident in adulthood. Future studies will focus on further defining the major cellular and molecular mechanisms mediating CNS environmental changes following developmental ablation of mature oligodendrocyte.

Declaration of competing interest

We do not have any conflict of interest regarding this study.

Acknowledgments

This work was supported by NS30800 and the Vivian Gill Endowment from The George Washington University and imaging was performed at the George Washington University Nanofabrication and Imaging Center (GWNIC).

References

Bilbo, S.D., et al., 2005. Neonatal infection induces memory impairments following an immune challenge in adulthood. Behav. Neurosci. 119 (1), 293–301.
Boisse, L., et al., 2004. Long-term alterations in neuroimmune responses after neonatal exposure to lipopolysaccharide. J. Neurosci. 24 (21), 4928–4934.
Caprariello, A.V., et al., 2012. Apoptosis of oligodendrocytes in the central nervous system results in rapid focal demyelination. Ann. Neurol. 72 (3), 395–405.
Caprariello, A.V., et al., 2015. Apoptosis of oligodendrocytes during early development delays myelination and impairs subsequent responses to demyelination. J. Neurosci. 35 (41), 14031–14041.
Cunningham, C., et al., 2009. Systemic inflammation induces acute behavioral and cognitive changes and accelerates neurodegenerative disease. Biol. Psychiatr. 65 (4), 304–312.
Dietert, R.R., Dietert, J.M., Dewitt, J.C., 2011. Environmental risk factors for autism. Emerg. Health Threats J. 4, 7111.
Eagleton, M.J., et al., 2002. Southern Association for Vascular Surgery William J. von Leibig Award. Inflammation and intimal hyperplasia associated with experimental pulmonary embolism. J. Vasc. Surg. 36 (3), 581–588.
Fenn, A.M., et al., 2014. Immune activation promotes depression 1 month after diffuse brain injury: a role for primed microglia. Biol. Psychiatr. 76 (7), 575–584.
Gluckman, P.D., et al., 2008. Effect of in utero and early-life conditions on adult health and disease. N. Engl. J. Med. 359 (1), 61–73.
Hanamsagar, R., Bilbo, S.D., 2017. Environment matters: microglia function and dysfunction in a changing world. Curr. Opin. Neurobiol. 47, 146–155.
Kamel, F.O., 2019. Factors involved in relapse of multiple sclerosis. J Microsc Ultrastruct 7 (3), 103–108.
Kiernan, E.A., et al., 2016. Mechanisms of microglial activation in models of inflammation and hypoxia: implications for chronic intermittent hypoxia. J. Physiol. 594 (6), 1563–1577.
Kotter, M.R., et al., 2006. Myelin impairs CNS remyelination by inhibiting oligodendrocyte precursor cell differentiation. J. Neurosci. 26 (1), 328–332.
Lefeuvre, J.A., et al., 2019. The spectrum of spinal cord lesions in a primate model of multiple sclerosis. Mult. Scler. 26 (3), 284–293, 1352458518822408.
Locatelli, G., et al., 2012. Primary oligodendrocyte death does not elicit anti-CNS immunity. Nat. Neurosci. 15 (4), 543–550.
McCarthy, D.P., Richards, M.H., Miller, S.D., 2012. Mouse models of multiple sclerosis: experimental autoimmune encephalomyelitis and Theiler's virus-induced demyelinating disease. Methods Mol. Biol. 900, 381–401.
Mueller, R.B., et al., 2007. Attraction of phagocytes by apoptotic cells is mediated by lysophosphatidylcholine. Autoimmunity 40 (4), 342–344.
Nakatsuji, Y., Miller, R.H., 2001. Density dependent modulation of cell cycle protein expression in astrocytes. J. Neurosci. Res. 66 (3), 487–496.
Nakatsuji, Y., Miller, R.H., 2001. Control of oligodendrocyte precursor proliferation mediated by density-dependent cell cycle protein expression. Dev. Neurosci. 23 (4–5), 356–363.
Novotna, K., et al., 2019. Why patients with multiple sclerosis perceive improvement of gait during treatment with natalizumab? J. Neural. Transm. 126 (6), 731–737. Vienna.
Ogura, H., et al., 1999. Priming, second-hit priming, and apoptosis in leukocytes from trauma patients. J. Trauma 46 (5), 774–781 discussion 781-3.
Pajoohesh-Ganji, A., Miller, R.H., 2016. Oligodendrocyte ablation as a tool to study demyelinating diseases. Neural Regen Res 11 (6), 886–889.
Pajoohesh-Ganji, A., Miller, R.H., 2019. Targeted oligodendrocyte apoptosis in optic nerve leads to persistent demyelination. Neurochem. Res. 45 (3), 580–590.
Pierson, E., et al., 2012. Mechanisms regulating regional localization of inflammation during CNS autoimmunity. Immunol. Rev. 248 (1), 205–215.
Plemel, J.R., et al., 2013. Myelin inhibits oligodendroglial maturation and regulates oligodendrocytic transcription factor expression. Glia 61 (9), 1471–1487.
Polter, A., et al., 2010. Deficiency in the inhibitory serine-phosphorylation of glycogen synthase kinase-3 increases sensitivity to mood disturbances. Neuropsychopharmacology 35 (8), 1761–1774.
Quarles, R.H., 2007. Myelin-associated glycoprotein (MAG): past, present and beyond. J. Neurochem. 100 (6), 1431–1448.
Ravichandran, K.S., 2010. Find-me and eat-me signals in apoptotic cell clearance: progress and conundrums. J. Exp. Med. 207 (9), 1807–1817.
Robinson, S., Miller, R.H., 1999. Contact with central nervous system myelin inhibits oligodendrocyte progenitor maturation. Dev. Biol. 216 (1), 359–368.
Sonnenberg, A., Ajdacic-Gross, V., 2018. Similar birth-cohort patterns in Crohn's disease and multiple sclerosis. Mult. Scler. 24 (2), 140–149.
Syed, Y.A., et al., 2008. Inhibition of oligodendrocyte precursor cell differentiation by myelin-associated proteins. Neurosurg. Focus 24 (3–4), E5.
Traka, M., et al., 2016. Oligodendrocyte death results in immune-mediated CNS demyelination. Nat. Neurosci. 19 (1), 65–74.
Tyurin, V.A., et al., 2014. Oxidatively modified phosphatidylserines on the surface of apoptotic cells are essential phagocytic 'eat-me' signals: cleavage and inhibition of phagocytosis by Lp-PLA2. Cell Death Differ. 21 (5), 825–835.
Witcher, K.G., Eiferman, D.S., Godbout, J.P., 2015. Priming the inflammatory pump of the CNS after traumatic brain injury. Trends Neurosci. 38 (10), 609–620.